Current- and field-driven magnetic antivortices

André Drews,[1] Benjamin Krüger,[2] Markus Bolte,[1] and Guido Meier[1]
[1]*Institut für Angewandte Physik und Zentrum für Mikrostrukturforschung, Universität Hamburg, Jungiusstrasse 11, 20355 Hamburg, Germany*
[2]*I. Institut für Theoretische Physik, Universität Hamburg, Jungiusstrasse 9, 20355 Hamburg, Germany*
(Received 4 July 2007; revised manuscript received 25 January 2008; published 17 March 2008)

Antivortices in ferromagnetic thin-film elements are in-plane magnetization configurations with a core pointing perpendicular to the plane. By using micromagnetic simulations, we find that magnetic antivortices gyrate on elliptical orbits similar to magnetic vortices when they are excited by alternating magnetic fields or by spin-polarized currents. The phase between high-frequency excitation and antivortex gyration is investigated. In the case of excitation by spin-polarized currents, the phase is determined by the polarization of the antivortex, while for excitation by magnetic fields, the phase depends on the polarization and in-plane magnetization. Simultaneous excitation by a current and a magnetic field can lead to a maximum enhancement or to an entire suppression of the amplitude of the core gyration, depending on the angle between the excitation and the in-plane magnetization. This variation of the amplitude can be used to experimentally distinguish between the spin-torque and Oersted-field driven motion of an antivortex core.

DOI: 10.1103/PhysRevB.77.094413 PACS number(s): 75.60.Ch, 72.25.Ba, 76.50.+g

I. INTRODUCTION

Magnetic vortices and antivortices exist in ferromagnetic thin-film elements, where the interplay of demagnetization and exchange energy forces the magnetization out of plane to form a core in the center.[1,2] The orientation of the vortex or antivortex core, which is denoted as the polarization p, is highly interesting for technical applications, e.g., magnetic memory devices, as it can be binary coded.[3,4] Magnetic vortices have been intensively studied in the past few years. It has been shown that a vortex core is deflected from its equilibrium position when excited by magnetic fields or spin-polarized currents.[5,6] The deflection causes a magnetic stray field, which, in turn, exerts a force on the core.[7,8] The resulting gyroscopic motion can be described by a damped two-dimensional harmonic oscillator.[9]

The dynamics of magnetic antivortices has heretofore not been studied as intensively as magnetic vortex dynamics. Antivortices appear, e.g., in cross-tie domain walls, and individual antivortices have been found in clover-shaped samples.[3,10–12] As illustrated in Fig. 1, their in-plane magnetization shows a twofold rotational symmetry that is different from the continuous rotational symmetry of a vortex state. Due to their different in-plane magnetizations, antivortex dynamics differs from vortex dynamics, as is shown in this paper. An understanding of the dynamics of both antivortices and vortices is crucial for the description of vortex-antivortex creation and annihilation. These processes have recently received a lot of attention as they are predominant features in the motion of cross-tie walls and in the switching of vortex cores.[3,13–16]

Here, we investigate the dynamics of antivortex cores, i.e., sense, phase, and amplitude of gyration, and compare them to the dynamics of magnetic vortices. We show that the direction of the in-plane magnetization around the (anti)vortex core determines the phase between the exciting alternating magnetic field and the deflection of the (anti)vortex core. For spin-polarized alternating currents, the direction of the in-plane magnetization has no effect on the phase. Both micromagnetic simulations and an analytical model show that simultaneous excitation by magnetic fields and spin-polarized currents can lead to an enhancement or to an entire suppression of the antivortex core displacement.

To classify vortices and antivortices, the in-plane magnetization can be described by the relation[17]

$$\phi = n\beta + \phi_0 \tag{1}$$

between the angular coordinate of the local in-plane magnetization ϕ and the angle β in real space with respect to the center of the (anti)vortex core, as shown in Fig. 1. The angles ϕ and β follow the mathematical sense of rotation. For a vortex, $n=1$, such that the in-plane magnetization turns in the same direction as the angle in real space with a constant difference ϕ_0 between ϕ and β. For vortices, the angle ϕ_0 is independent of the choice of the axis to which β and ϕ are measured. Thus, for vortices, ϕ_0 is an intrinsic quantity which can be expressed by the chirality c as $\phi_0 = c\pi/2$. In standard geometries and ferromagnetic materials, stable vortices can only possess the chiralities $c=1$ or $c=-1$. They can be mapped onto each other by mirroring the sample. For an antivortex, $n=-1$. This means that the in-plane magnetization turns opposite to the angle in real space. Although for antivortices the angle ϕ_0 is generally not conserved because the rotations of the sample lead to different values, we define

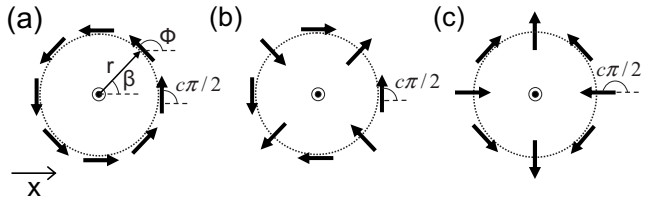

FIG. 1. Definition of $c=2/\pi\cdot(\phi-n\beta)$ for vortices and antivortices by Eq. (1). (a) Magnetic vortex ($n=1$) with $c=1$. (b) Antivortex ($n=-1$) with $c=1$. (c) Antivortex ($n=-1$) with $c=2$.

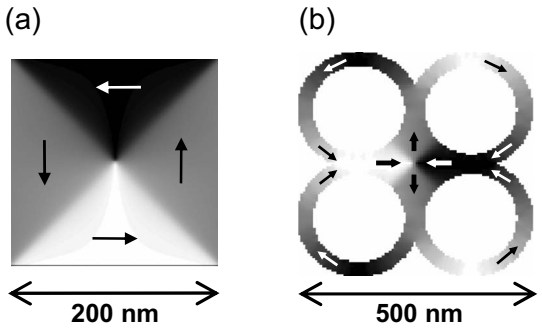

FIG. 2. Size and shape of (a) the vortex and (b) the antivortex samples.

a quantity $c=2\phi_0/\pi$ for antivortices with respect to a distinct axis.[18] Antivortices exhibit values c in the interval $(-2,2]$. A rotation of the antivortex by an angle Θ leads to a change in the c value of $c=2\Theta$. This is due to the twofold symmetry of the in-plane magnetization of an antivortex.

II. MICROMAGNETIC SIMULATIONS

To simulate magnetic-field induced antivortex dynamics, the OOMMF (Ref. 19) code sped up by higher order Runge–Kutta algorithms is used. The extended code[21] includes the spin-torque terms in the Landau–Lifshitz–Gilbert equation, as given by Zhang and Li[20]

$$\frac{d\boldsymbol{M}}{dt} = -\gamma'\boldsymbol{M}\times\left(\boldsymbol{H}_{\text{eff}}+\frac{\alpha}{M_S}\boldsymbol{M}\times\boldsymbol{H}_{\text{eff}}\right)-(1+\alpha\xi)\frac{b_j'}{M_s^2}\boldsymbol{M}$$
$$\times[\boldsymbol{M}\times(\boldsymbol{j}\cdot\nabla)\boldsymbol{M}]-(\xi-\alpha)\frac{b_j'}{M_s}\boldsymbol{M}\times(\boldsymbol{j}\cdot\nabla)\boldsymbol{M}. \quad (2)$$

Here, $\gamma'=\gamma/(1+\alpha^2)$, where γ is the gyromagnetic ratio, α is the Gilbert damping, and ξ is the ratio between exchange and spin-flip relaxation times. The coupling between the local current $\boldsymbol{j}$ and magnetization $\boldsymbol{M}$ is represented by $b_j'=\mu_B P/[eM_s(1+\alpha^2)]$, where P is the spin polarization. We simulate the excitation of a vortex in a $200\times200\times20$ nm^3 Permalloy square and an antivortex in a $500\times500\times40$ nm^3 clover-shaped sample. The two geometries are shown in Fig. 2. Different thicknesses of $t=20$ nm for the vortex and $t=40$ nm for the antivortex samples are chosen in order to obtain similar eigenfrequencies for the two geometries. We assume a saturation magnetization $M_s=8.6\times10^5$ A/m, an exchange constant $A=1.3\times10^{-11}$ J/m, a Gilbert damping parameter $\alpha=0.01$, and a ratio $\xi=0.9\alpha$ between exchange and spin-flip relaxation times.[22,23] A lateral cell size of 4 nm is used. Thus, the cell size is below the exchange length of Permalloy of $l_{\text{ex}}=\sqrt{2A/\mu_0 M_s^2}\approx5.3$ nm. The position of the core is defined as the position of the maximum out-of-plane magnetization. To increase the spatial resolution, the magnetization of adjacent cells is matched by a polynomial of the second order.[9]

III. EXCITATION BY MAGNETIC FIELD AND SPIN-POLARIZED CURRENT

The eigenfrequencies of vortex and antivortex are determined by exciting the core with a current. The free relaxation

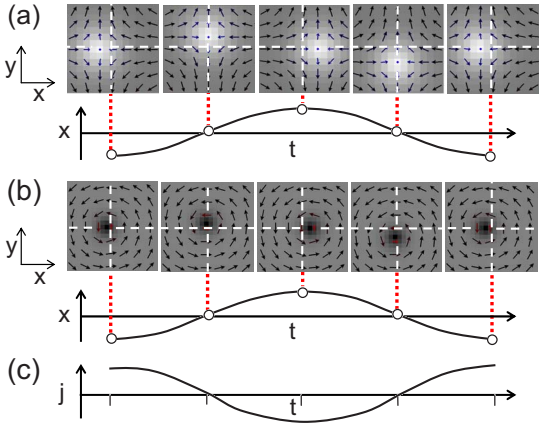

FIG. 3. (Color online) Simulation of one gyration period of (a) an antivortex and (b) a vortex. Both have the topological charge $q=-1/2$ and are excited at the resonance frequency (727 MHz for the antivortex and 742 MHz for the vortex) by a current of amplitude $jP=1.5\times10^{10}$ A/m^2. The graphs below the magnetization images show the deflection in the x direction. (c) Exciting alternating current.

of the magnetization yields the free frequency ω_f and damping Γ of the vortex or antivortex. Because the damping is small compared to the free frequency ($\Gamma\ll\omega_f$), the antivortex and vortex are weakly damped systems. Thus, the frequency of the free oscillation ω_f and the resonance frequency ω_r are approximately the same. The simulated gyration of an antivortex core [$p=1$, see Fig. 3(a)] and a vortex core [$p=-1$, see Fig. 3(b)], which are both driven by an ac current of amplitude $jP=1.5\times10^{10}$ A/m^2, are shown in Fig. 3. They both possess the same sense of gyration as defined by the topological charge,[24–26] i.e., $q=np/2=-1/2$. It is known that vortices gyrate counterclockwise with a positive polarization and clockwise with a negative polarization.[5] On the other hand, antivortices gyrate clockwise with a positive polarization and counterclockwise with a negative polarization. This is directly observed in the simulations. For small current or small magnetic field amplitudes, the simulated displacement of the antivortex is found to linearly increase with the increasing excitation amplitude. This is due to the harmonic potential of the domains' stray field for small displacements of the antivortex core. Thus, there is a linear restoring force on the antivortex, which has also been found for a vortex.[9]

To obtain the resonance curve for the amplitude and the phase η of the antivortex core, either the sinusoidal currents or the magnetic fields of frequencies at, above, and below the resonance frequency ω_r are applied. Throughout this paper, the current is applied in the x direction, while the magnetic field is applied in the y direction. The resonance curve of a harmonic oscillator[27] with a resonance frequency $\omega_r/2\pi=727$ MHz and a damping $\Gamma/2\pi=6.4$ MHz matches the numerical data very well, as shown in Figs. 4(a) and 4(b). In general, the antivortex gyrates on elliptical orbits. The semimajor (semiminor) axis of the ellipses at frequencies below resonance changes into the semiminor (semimajor) axis at frequencies above resonance. At resonance, the trajectories are circular. This is illustrated in Fig. 4(a) for a current-

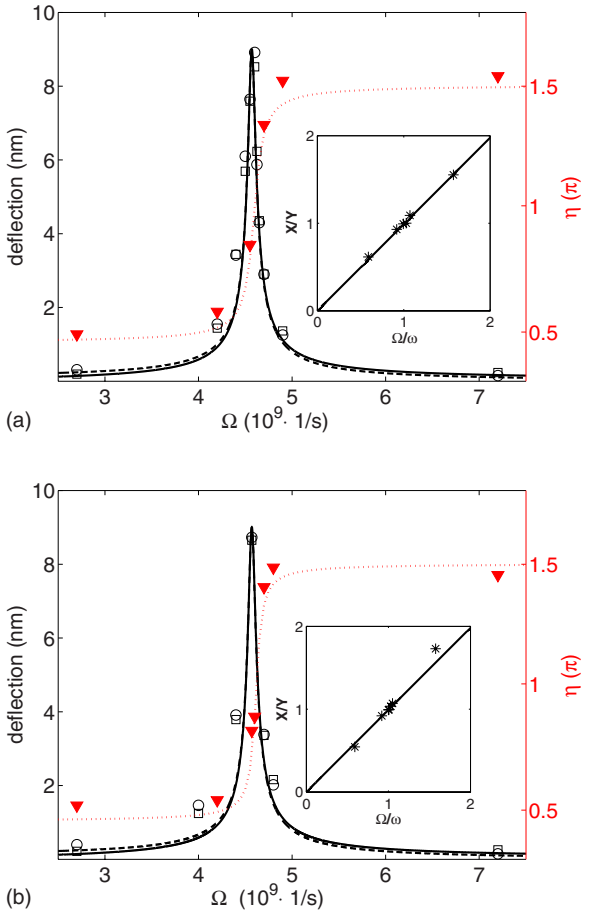

FIG. 4. (Color online) Exemplary resonance curves for the semiaxes of the elliptical trajectories and the phase η of an antivortex core gyration excited by (a) a current of amplitude $jP=1.5\times10^{10}$ A/m^2 ($c=2$) and (b) a magnetic field of amplitude $H=300$ A/m ($c=0$). The symbols are the results from micromagnetic simulations. The open squares illustrate the semiaxes in the x direction and the open circles illustrate the semiaxes in the y direction. The triangles show the phase η. The asterisks illustrate the ratio between the semiaxes x and y. The solid line is the x component and the dashed line is the y component of the amplitude of a fitted resonance curve of a harmonic oscillator. The dotted red line is a fit of the phase η. The insets show fits of the ratio between the semiaxes x and y as a function of the frequency.

driven antivortex with $c=2$ and in Fig. 4(b) for a magnetic-field driven antivortex with $c=0$. For both, the semimajor axes point in the y direction at frequencies below resonance and in the x direction at frequencies above resonance.

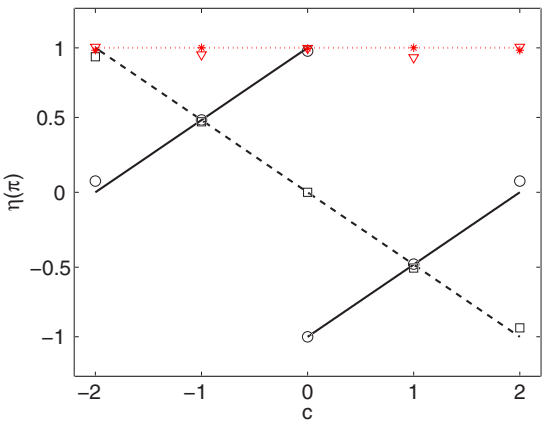

FIG. 5. (Color online) Phase η between excitation and displacement for an antivortex core gyration at resonance. The dotted red line illustrates the phase when the antivortex core is excited by a spin-polarized current. The asterisks represent corresponding results from micromagnetic simulations for positive core polarization ($p=1$) and the triangles for negative polarization ($p=-1$). For excitation with a magnetic field, the solid line illustrates the phase for positive core polarization ($p=1$) and the dashed black line illustrates the phase for negative polarization ($p=-1$). The numerical results are depicted by open circles and squares.

The phase η is defined by the temporal delay between the maximum of the applied current or field and the maximum core displacement in the x direction. As in the case of a harmonic oscillator, the phase η changes by π when the exciting frequency Ω is increased from values well below to values well above the resonance frequency ω_r. This is illustrated in Fig. 4(a) for current and in Fig. 4(b) for magnetic-field excitation.

We numerically simulate the dependence of the phase on the direction of the in-plane magnetization by exciting at resonance antivortices of all possible integer c values and of both polarizations $p=-1$ and $p=1$. For current excitation, for all c-values, the antivortex cores are deflected into the physical current direction ($\eta=\pi$). For magnetic field excitation, the phase is found to depend on the direction of the in-plane magnetization, as shown in Fig. 5. For a constant frequency, the phase varies by 2π when c is changed from -2 to 2, i.e., when the sample is rotated by π with respect to the magnetic field. At resonance, the phase changes from 0 to 2π for $p=1$ and from π to $-\pi$ for $p=-1$, as illustrated in Fig. 5.

The phase η and its dependence on the direction of the in-plane magnetization are analytically studied by using the equation of motion for vortices and antivortices[27] assuming low damping ($\omega_r \gg \Gamma$). The equation for the deflection

$$\begin{pmatrix} x \\ y \end{pmatrix} = -\chi \cdot \begin{pmatrix} v_H \sin\left(\frac{\pi c}{2}\right)\omega + \left[v_H p \cos\left(\frac{\pi c}{2}\right) + v_j\right] i\Omega \\ \left[v_H n \cos\left(\frac{\pi c}{2}\right) + v_j n p\right]\omega - v_H n p \sin\left(\frac{\pi c}{2}\right) i\Omega \end{pmatrix} \cdot e^{i\Omega t} \tag{3}$$

is derived from the equation of Thiele *et al.*[8] for excitation with magnetic fields and the extension by Thiaville[7] for spin-polarized currents. A harmonic potential due to the demagnetizing field is assumed.[27] The velocity due to the adiabatic spin-torque term is $v_j = b_j j_0$, the velocity due to the magnetic field is $v_H = \gamma H_0 l/(2\pi)$, and the susceptibility of a harmonic oscillator is $\chi = 1/[\omega^2 + (i\Omega + \Gamma)^2]$. Equation (3) states that a change of the c value leads to a rotation of the magnetic force. This, in turn, causes a dependence of the phase on the in-plane magnetization. For example, a change from $c=-1$ to $c=1$ is equivalent to a rotation of the magnetic force by an angle of π. At resonance, Eq. (3) yields the following deflection:

$$x(c,p,t) = \frac{v_H}{2\Gamma} e^{i\Omega t} e^{i\pi(1+p-pc)/2}. \tag{4}$$

The maximum excitation is reached for $i\Omega t = -i\pi\left(\frac{1+p-pc}{2}\right)$, such that the phase of the antivortex motion that is induced by a magnetic field at resonance reads

$$\eta_H = -\pi\left(\frac{1+p-pc}{2}\right). \tag{5}$$

For purely current-driven excitation, Eq. (3) gives

$$x(c,p,t) = -\frac{v_j}{2\Gamma} e^{i\Omega t}. \tag{6}$$

Hence, the phase induced by a current is $\eta_j = \pi$ at resonance. This means that for a current excitation, the phase is independent of the direction of the in-plane magnetization and polarization. Figure 5 demonstrates that the analytical results agree well with the simulations.

IV. AMPLITUDE VARIATION OF GYRATION

In the following, we simulate antivortices that are simultaneously excited by a magnetic field and a spin-polarized current. First, the antivortex is excited by a current in the x direction in the absence of a magnetic field. Then, the amplitude of a magnetic field in the y direction is tuned until the antivortex core gyration possesses the same amplitude as under current excitation. In our case, the core is excited by a spin-polarized current of amplitude $jP = 0.7 \times 10^{10}$ A/m^2 that corresponds to a magnetic field of amplitude $H = 122$ A/m. Then, the current and the magnetic field are simultaneously applied. Different directions of the in-plane magnetization (see Fig. 6) are chosen to investigate the c-dependent variation of the core amplitude for a positive polarization. The simulation shows a doubling of the amplitude at $c=0$ and a complete suppression at $c=2$. Thus, a superposition of the deflection by current and a perpendicular field leads to an amplitude variation in dependence on the direction of the in-plane magnetization of the sample. This is due to the c-dependent phase between antivortex core displacement and magnetic field [see Eq. (5)]. The forces due to the current and magnetic field are proportional to the deflections. If they are parallel or antiparallel, an enhancement or suppression of the core displacement is found, respectively.

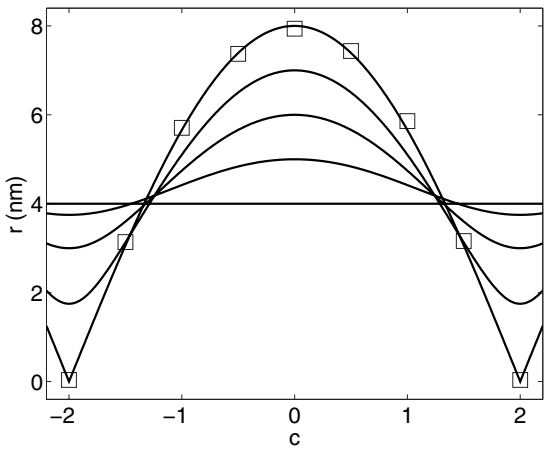

FIG. 6. Amplitude of displacement of an antivortex core with polarization $p=1$ at resonance. The antivortex is simultaneously excited by a magnetic field in the y direction and a current in the x direction. The symbols denote simulated results for $v_H = v_j$ and the lines are fits for different ratios v_H/v_j according to Eq. (7).

When both deflections have the same amplitude, the amplitude of gyration can be doubled or completely quenched, as shown in Fig. 6.

Using the addition theorem from Eq. (3), one can derive the c-dependent amplitude variation

$$r = r_0 \sqrt{\left(\frac{v_H}{v_j} - p\right)^2 \sin^2\left(\frac{\pi c}{4}\right) + \left(\frac{v_H}{v_j} + p\right)^2 \cos^2\left(\frac{\pi c}{4}\right)} \tag{7}$$

of the antivortex core gyration at resonance. This is a general expression for arbitrary ratios v_H/v_j between the antivortex core velocities due to the current and magnetic fields for both polarizations and all c values. The amplitude is plotted in Fig. 6.

An inhomogeneous current distribution in the direction of the film normal generates a nonzero Oersted field perpendicular to the current.[28] As experimental proof of the dependence of the amplitude on the direction of the in-plane magnetization, we propose a setup with a clover-shaped sample, which is illustrated in Fig. 7. A similar sample was investigated by Shigeto *et al.*[10] by means of magnetic-force microscopy. Excitation by a spin current in the x direction or y direction through electrical contacts corresponds to a direction of the in-plane magnetization for $c=2$ and $c=0$, respectively. For the polarization $p=1$, we expect a suppressed motion when the current is applied in the x direction and an enhanced amplitude when it is applied in the y direction. The variation of the amplitude for $c=0$ and $c=2$ could be used to determine the ratio between the forces on the antivortex core due to an Oersted field and a current.

V. CONCLUSION

In conclusion, we have demonstrated by micromagnetic simulations that antivortices excited by spin-polarized ac

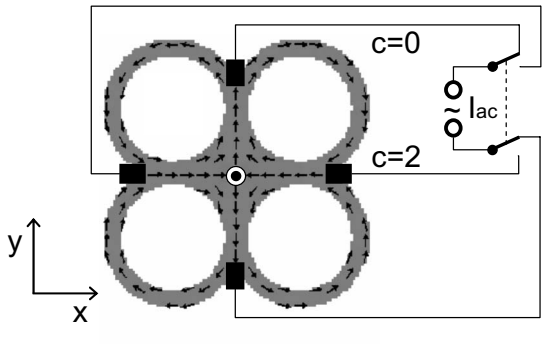

FIG. 7. Proposed setup with electrical contacts to excite a single antivortex, here with polarization $p=1$. The quantity c depends on the direction of the exciting ac. For current in the x or y direction, the deflection is suppressed or amplified, respectively.

currents or magnetic fields gyrate on elliptical orbits. These orbits can be described well by the analytical model of a two-dimensional harmonic oscillator. The sense of gyration of antivortices solely depends on the topological charge, i.e., $q=np/2$. The phase of the antivortex motion excited by an alternating magnetic field depends also on the direction of the in-plane magnetization. Antivortices that are simultaneously excited by a spin-polarized current and a magnetic field show an enhancement or a suppression of the deflection amplitude depending on the direction of the in-plane magnetization. The effect of the amplitude variation depending on the in-plane magnetization can be used to experimentally investigate the influence of Oersted fields in current-induced antivortex dynamics.

ACKNOWLEDGMENTS

We thank Ulrich Merkt and Daniela Pfannkuche for valuable discussions and encouragement. Financial support by the Deutsche Forschungsgemeinschaft via the Graduiertenkolleg 1286 "Functional metal-semiconductor hybrid systems" and via Sonderforschungsbereich 668 "Magnetismus vom Einzelatom zur Nanostruktur" is gratefully acknowledged.

[1] T. Shinjo, T. Okuno, R. Hassdorf, K. Shigeto, and T. Ono, Science **289**, 930 (2000).
[2] A. Wachowiak, J. Wiebe, M. Bode, O. Pietzsch, M. Morgenstern, and R. Wiesendanger, Science **298**, 577 (2002).
[3] Y. Liu, S. Gliga, R. Hertel, and C. M. Schneider, Appl. Phys. Lett. **91**, 112501 (2007).
[4] B. Van Waeyenberge, A. Puzic, H. Stoll, K. W. Chou, T. Tyliszczak, R. Hertel, M. Fähnle, H. Brückl, K. Rott, G. Reiss, I. Neudecker, D. Weiss, C. H. Back, and G. Schütz, Nature (London) **444**, 461 (2006).
[5] S.-B. Choe, Y. Acremann, A. Scholl, A. Bauer, A. Doran, J. Stöhr, and H. A. Padmore, Science **304**, 420 (2004).
[6] J. Shibata, Y. Nakatani, G. Tatara, H. Kohno, and Y. Otani, Phys. Rev. B **73**, 020403(R) (2006).
[7] A. A. Thiele, Phys. Rev. Lett. **30**, 230 (1973).
[8] A. Thiaville, Y. Nakatani, J. Miltat, and Y. Suzuki, Europhys. Lett. **69**, 990 (2005).
[9] B. Krüger, A. Drews, M. Bolte, U. Merkt, D. Pfannkuche, and G. Meier, Phys. Rev. B **76**, 224426 (2007).
[10] K. Shigeto, T. Okuno, K. Mibu, T. Shinjo, and T. Ono, Appl. Phys. Lett. **80**, 4190 (2002).
[11] Y. C. Chang, C. C. Chang, W. Z. Hsieh, H. M. Lee, and J. C. Wu, IEEE Trans. Magn. **41**, 959 (2005).
[12] H. Wang and C. E. Campbell, Phys. Rev. B **76**, 220407(R) (2007).
[13] R. Hertel and C. M. Schneider, Phys. Rev. Lett. **97**, 177202 (2006).
[14] A. Neudert, J. McCord, R. Schäfer, and L. Schultz, Phys. Rev. B **75**, 172404 (2007).
[15] S.-K. Kim, Y.-S. Choi, K.-S. Lee, K. Y. Guslienko, and D.-E. Jeong, Appl. Phys. Lett. **91**, 082506 (2007).
[16] K. Kuepper, M. Buess, J. Raabe, C. Quitmann, and J. Fassbender, Phys. Rev. Lett. **99**, 167202 (2007).
[17] J. He, Z. Li, and S. Zhang, Phys. Rev. B **73**, 184408 (2006).
[18] Here, we use the x axis as the distinct axis.
[19] OOMMF User's Guide, version 1.0, M. J. Donahue and D. G. Porter, Interagency Report No. NISTIR 6376, National Institute of Standards and Technology, Gaithersburg, MD, 1999 (http://math.nist.gov/oommf/).
[20] S. Zhang and Z. Li, Phys. Rev. Lett. **93**, 127204 (2004).
[21] B. Krüger, D. Pfannkuche, M. Bolte, G. Meier, and U. Merkt, Phys. Rev. B **75**, 054421 (2007).
[22] G. Meier, M. Bolte, R. Eiselt, B. Krüger, D.-H. Kim, and P. Fischer, Phys. Rev. Lett. **98**, 187202 (2007).
[23] M. Hayashi, L. Thomas, Ya. B. Bazaliy, C. Rettner, R. Moriya, X. Jiang, and S. S. P. Parkin, Phys. Rev. Lett. **96**, 197207 (2006).
[24] A. Abanov and V. L. Pokrovsky, Phys. Rev. B **58**, R8889 (1998).
[25] V. L. Golo and A. M. Perelomov, Lett. Math. Phys. **2**, 477 (1978).
[26] O. A. Tretiakov and O. Tchernyshyov, Phys. Rev. B **75**, 012408 (2007).
[27] B. Krüger, A. Drews, M. Bolte, U. Merkt, D. Pfannkuche, and G. Meier, J. Appl. Phys. **103**, 07A501 (2008).
[28] M. Bolte, G. Meier, B. Krüger, A. Drews, R. Eiselt, L. Bocklage, S. Bohlens, T. Tyliszczak, A. Vansteenkiste, B. Van Waeyenberge, K. W. Chou, A. Puzic, and H. Stoll (unpublished).